

PENETRATION OF SOLAR RADIATION IN THE SCHUMANN-RUNGE BANDS OF MOLECULAR OXYGEN

G. KOCKARTS

Institut d'Aéronomie Spatiale de Belgique, Brussels, Belgium

Molecular oxygen is subject to photodissociation leading to a production of oxygen atoms which are involved in numerous aeronomic reactions below 100 km. Among several band systems, the Schumann-Runge bands $B\ ^3\Sigma_u^- - X\ ^3\Sigma_g^-$ are of fundamental importance in the chemosphere since they are situated in a wavelength region (1750 Å–2050 Å) where the solar radiation can penetrate deeply into the Earth's atmosphere.

In the thermosphere, atomic oxygen is produced mainly by photodissociation of O_2 in the Schumann-Runge continuum ($\lambda < 1750 \text{ \AA}$). In the stratosphere and mesosphere, molecular oxygen is photodissociated by radiation between 2424 Å and 1750 Å, i.e. in the spectral region of the Herzberg continuum and of the Schumann-Runge bands. Since predissociation occurs in the Schumann-Runge bands (Flory, 1936), an additional source of $O(^3P)$ atoms produced in the Herzberg continuum is available in the mesosphere. The effects of this process have been investigated by Hudson and Carter (1969), by Hudson *et al.* (1969) and by Brinkmann (1969). Recent absorption cross section measurements (Ackerman *et al.*, 1969) and the determination of the structure of the 0–0 to the 13–0 Schumann-Runge bands (Ackerman and Biaumé, 1970) made it possible to compute the O_2 absorption cross sections at very close intervals over the whole Schumann-Runge system (Ackerman *et al.*, 1970). The depth of the penetration of solar radiation into the chemosphere can be determined with these new data. It is of importance to know the fine structure of the absorption in the Schumann-Runge bands, especially when minor constituents are studied by absorption techniques. Jursa *et al.* (1959) attempted to detect nitric oxide in the altitude range 60 to 90 km and obtained in situ absorption spectra of the O_2 Schumann-Runge bands which clearly show the importance of the rotational structure. At 63 km altitude they even observed with certainty the 1–0 band and at 87 km the bands extend to $v' = 13$.

The numerical method and the experimental data used for the computation of the absorption cross section every 0.5 cm^{-1} from the 19–0 to the 0–0 band are described by Ackerman *et al.* (1970). Figure 1 gives a summary of the computations performed at 300 K. Experimental cross sections obtained by Ackerman *et al.* (1969) are indicated by crosses. It can be seen that the $v'' = 1$ bands have to be taken into account in the overall absorption. Also, the overlapping of the rotational lines within a specific band cannot be neglected in order to get theoretical cross sections which fit the experimental values obtained at precisely known wavelengths of silicon emission lines (Ackerman *et al.*, 1969). As the rotational line widths range between 0.5 cm^{-1} and 3.7 cm^{-1} (Ackerman and Biaumé, 1970), an experimental cross section can in fact be situated in the wing of a specific rotational line, and moreover the cross section changes

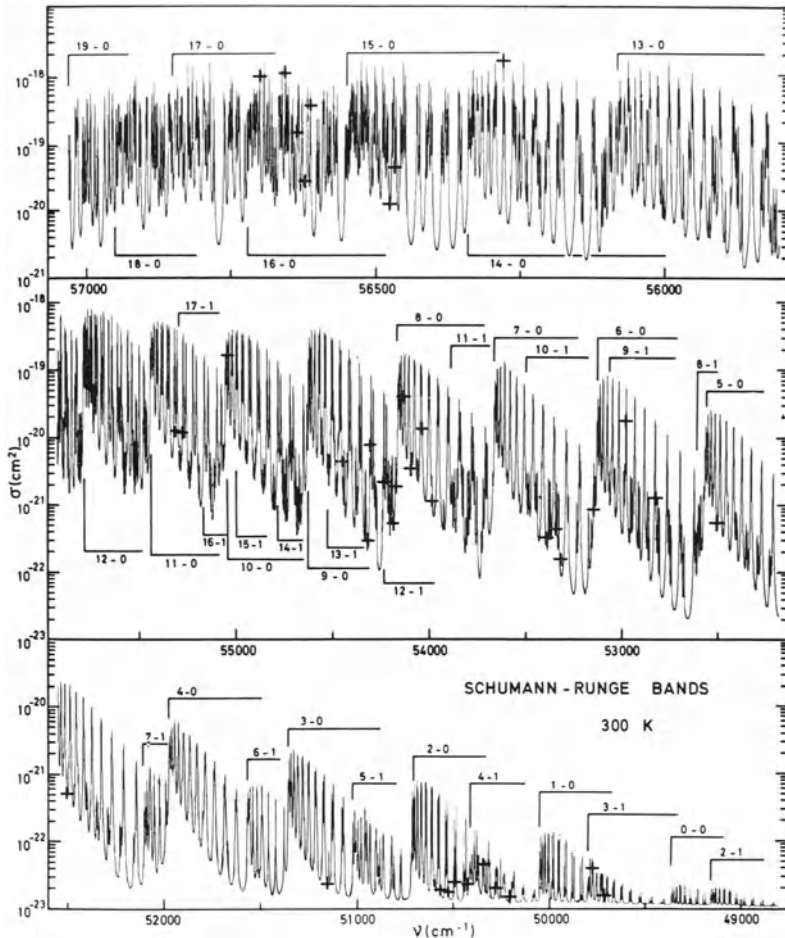


Fig. 1. Absorption cross sections of molecular oxygen at 300 K. Experimental values of Ackerman *et al.* (1969) are indicated by crosses (+).

by more than an order of magnitude over a rotational line. It was therefore necessary to compute the cross section every 0.5 cm^{-1} between 57030.5 cm^{-1} (1753.45 Å) and 48767.5 cm^{-1} (2050.55 Å) by taking into account the overlapping of all the lines having their maximum intensity within an interval of 150 cm^{-1} centred on each wave number. This means that the absorption contribution of the broadest rotational lines in the 4-0 band is taken into account up to 20 line widths from the center of the line. In such a way, more than 16000 absorption cross sections were obtained in the range of the Schumann-Runge bands for different temperatures. Table I gives average values over 500 cm^{-1} ($\sim 20 \text{ Å}$) of the absorption cross sections for 160 K, 200 K and 300 K. The wave number intervals were chosen only for convenience of presentation in other sections of this paper. The contribution of the Herzberg continuum is included in the computations and Table I shows that this contribution becomes more and more

TABLE I
Average absorption cross sections σ for different temperatures

$\nu(\text{cm}^{-1})$	$\lambda(\text{\AA})$	$\sigma(\text{cm}^2)$ $T = 300\text{K}$	$\sigma(\text{cm}^2)$ $T = 200\text{K}$	$\sigma(\text{cm}^2)$ $T = 160\text{K}$
57000–56500	1754.4–1769.9	1.28×10^{-19}	1.50×10^{-19}	1.57×10^{-19}
56500–56000	1769.9–1785.7	1.18	1.19	1.18
56000–55500	1785.7–1801.8	7.37×10^{-20}	6.47×10^{-20}	6.06×10^{-20}
55500–55000	1801.8–1818.2	4.77	5.05	5.21
55000–54500	1818.2–1834.9	3.16	3.02	2.94
54500–54000	1834.9–1851.8	1.61	1.40	1.33
54000–53500	1851.8–1869.2	8.74×10^{-21}	7.57×10^{-21}	7.25×10^{-21}
53500–53000	1869.2–1886.8	4.19	3.48	3.40
53000–52500	1886.8–1904.8	1.90	1.44	1.37
52500–52000	1904.8–1923.1	9.48×10^{-22}	6.04×10^{-22}	4.84×10^{-22}
52000–51500	1923.1–1941.8	6.24	5.72	5.72
51500–51000	1941.8–1960.8	2.15	1.87	1.87
51000–50500	1960.8–1980.2	7.56×10^{-23}	5.40×10^{-23}	5.42×10^{-23}
50500–50000	1980.2–2000.0	3.06	1.83	1.77
50000–49500	2000.0–2020.2	1.94	1.54	1.49

important for $\nu < 51500 \text{ cm}^{-1}$ since in this wave number region the absorption cross section due to the continuum is of the order of $1.3 \times 10^{-23} \text{ cm}^2$.

Within their limits of experimental error, Hudson and Carter (1969) could detect no significant change in the absorption cross sections when the temperature varies between 200K and 300K. Table I shows a ratio of the order of two for the average cross section in the interval 52500 cm^{-1} – 52000 cm^{-1} when the temperature decreases from 300K to 160K. A slight increase of the average cross section can even be seen towards shorter wavelengths. This behaviour can be explained by considering the factors responsible for a temperature effect. Firstly, the absorption cross section depends on the relative population of the first excited vibrational level $v''=1$ of the ground state. When the temperature decreases, the $v''=1$ bands shown in Figure 1 tend to disappear and, in the interval 52500 cm^{-1} – 52000 cm^{-1} , the 7–1 band is practically negligible at 160K. Secondly, the absorption cross section is influenced by the relative intensities of the rotational lines of the *P* and *R* branches inside a specific band. When an *average* cross section is then obtained over a certain interval, this effect is practically smoothed out and the average value can even slightly increase due to a different rotational distribution. However, when the cross sections are considered with a wave number resolution of the order of 0.5 cm^{-1} , the temperature effect is quite large and, at certain specific wave numbers, changes of the order of two are obtained between 300K and 200K. Some of the experimental values of Ackerman *et al.* (1969) could be fitted only with a 300K theoretical spectrum and not with a 200K spectrum (Ackerman *et al.*, 1970). Temperature-dependent absorption cross sections will therefore be used in the subsequent sections of this paper.

The penetration of the solar radiation into the atmosphere is limited by the optical depth, which in turn depends on the nature and the total content of the absorbing

species. In the lower thermosphere and mesosphere, molecular oxygen is the principal constituent responsible for the absorption in the Schumann-Runge spectral region. In the stratosphere, however, it is not possible to neglect the absorption by ozone since at 50 km the optical depth of ozone varies between 1×10^{-2} and 5×10^{-2} in the Schumann-Runge band region and increases rapidly in the Herzberg continuum. The presence of ozone affects strongly the rate of dissociation of O₂ below the stratopause (Nicolet, 1964) and the O₃ absorption has to be taken into account for the total optical depth in the Schumann-Runge bands. Table II gives the oxygen and ozone concentrations used in the following computations. This model has been deduced by Nicolet (1970) for the analysis of the ozone and hydrogen reactions in the chemosphere and it corresponds to daytime conditions.

TABLE II
Temperature, oxygen and ozone concentrations and their total contents

<i>z</i> (km)	<i>T</i> (K)	<i>n(O₂)</i> (cm ⁻³)	<i>n(O₃)</i> (cm ⁻³)	$\int_z^{\infty} n(O_2) dz$ (cm ⁻²)	$\int_z^{\infty} n(O_3) dz$ (cm ⁻²)
15	210.8	8.14×10^{17}	1.10×10^{12}	5.07×10^{23}	6.59×10^{18}
20	218.9	3.55	2.90	2.30	5.54
25	227.1	1.60	3.25	1.08	3.96
30	235.2	7.43×10^{16}	2.90	5.19×10^{22}	2.40
35	251.7	3.47	2.00	2.59	1.19
40	268.2	1.70	1.00	1.36	4.37×10^{17}
45	274.5	8.92×10^{15}	3.17×10^{11}	7.30×10^{21}	1.38
50	274.0	4.84	1.00	3.96	4.39×10^{16}
55	273.6	2.62	3.17×10^{10}	2.14	1.40
60	252.8	1.50	1.01	1.14	4.50×10^{15}
65	231.9	8.19×10^{14}	3.18×10^9	5.70×10^{20}	1.49
70	211.2	4.23	1.01	2.68	5.42×10^{14}
75	194.2	2.02	3.20×10^8	1.18	2.41
80	177.2	9.00×10^{13}	1.40	4.79×10^{19}	1.35
85	160.3	3.71	1.00	1.77	7.89×10^{13}
90	176.7	1.25	1.10	6.48×10^{18}	2.64
95	193.0	4.67×10^{12}	1.33×10^7	2.51	3.16×10^{12}
100	209.2	1.89	1.58×10^6	9.80×10^{17}	3.93×10^{11}
105	230.9	6.50×10^{11}	2.00×10^5	4.03	5.36×10^{10}
110	261.9	2.85	2.70×10^4	1.80	8.10×10^9
115	293.0	1.10	4.00×10^3	8.85×10^{16}	2.14

As molecular oxygen cross sections are now available every 0.5 cm⁻¹ in the Schumann-Runge bands (Ackerman *et al.*, 1970), it is possible to define an optical depth τ_i at height *z* for 0.5 cm⁻¹ intervals by the relation

$$\tau_i = \int_z^{\infty} \sigma_i(O_2) n(O_2) dz + \sigma(O_3) \int_z^{\infty} n(O_3) dz \quad (1)$$

where *n(O₂)* and *n(O₃)* are the molecular oxygen and the ozone concentrations, respectively. The ozone absorption cross section $\sigma(O_3)$ is taken as a constant over each

500 cm^{-1} interval given in Table I. The numerical values for $\sigma(\text{O}_3)$ are those adopted by Ackerman (1971). Since the absorption cross section for molecular oxygen is temperature dependent, it is necessary to introduce $\sigma_i(\text{O}_2)$ in (1) under the integral sign. The optical depths defined by (1) correspond to an overhead sun and have been computed over the whole Schumann-Runge system with a wave number resolution of 0.5 cm^{-1} and a height resolution of 1 km. Figure 2 shows the optical depth obtained at 60 km altitude between 1818 \AA and 1835 \AA . The 10-0 and 9-0 band origins are respectively at 55050.90 cm^{-1} and 54622.17 cm^{-1} and the absorption structure due to the *P* and *R* branches of these bands is visible in Figure 2. In particular, the doublet structure in the 10-0 band results from the relative situation of the alternate triplets *P* and *R*: $7P$ at 54966.9 cm^{-1} and $9R$ at 54990.4 cm^{-1} ; $9P$ at 54966.8 cm^{-1} and $11R$ at 54958.8 cm^{-1} ; $11P$ at 54930.1 cm^{-1} and $13R$ at 54920.8 cm^{-1} . The 15-1 and 14-1 bands fall also in the wave number region of Figure 2, and their effect is strongly apparent between 54800 cm^{-1} and 54650 cm^{-1} where the optical depth is less than unity. The $v''=1$ bands practically disappear below 200 K, but at 60 km they contribute to the optical thickness since the principal contribution arises from a region extending to a few scale heights above 60 km where the temperature is high enough. It is only at mesopause levels ($T < 200\text{ K}$) that the $v''=1$ bands are less efficient for the absorption, although it should be realized that the optical depth results from an effect which depends on an integration of the combined variation of $n(\text{O}_2)$ and $\sigma_i(\text{O}_2)$ over a range of heights. Figure 3 shows a similar behaviour at 40 km altitude between 1887 \AA and 1905 \AA . The structure results from the 6-0 and 5-0 bands for which the band origins are

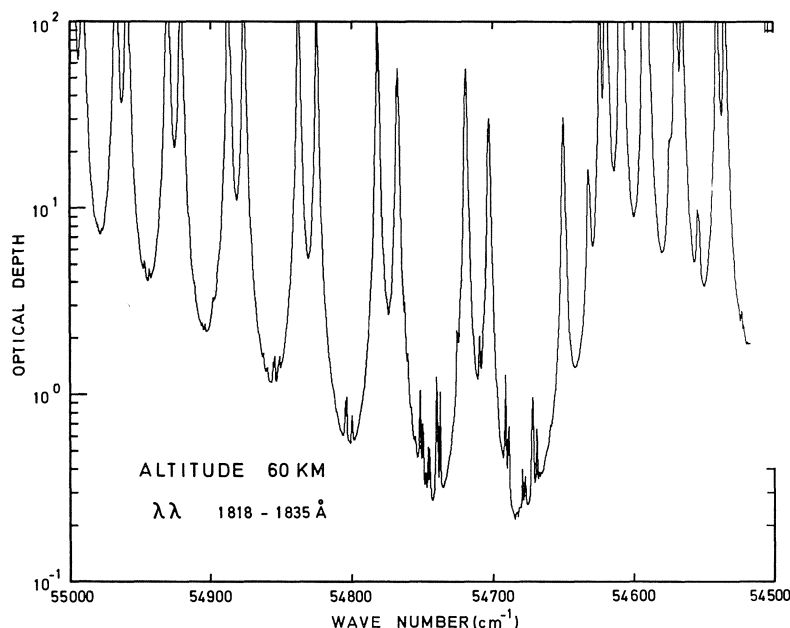


Fig. 2. Optical depth between 1818 \AA and 1835 \AA at 60 km. Resolution 0.5 cm^{-1} .

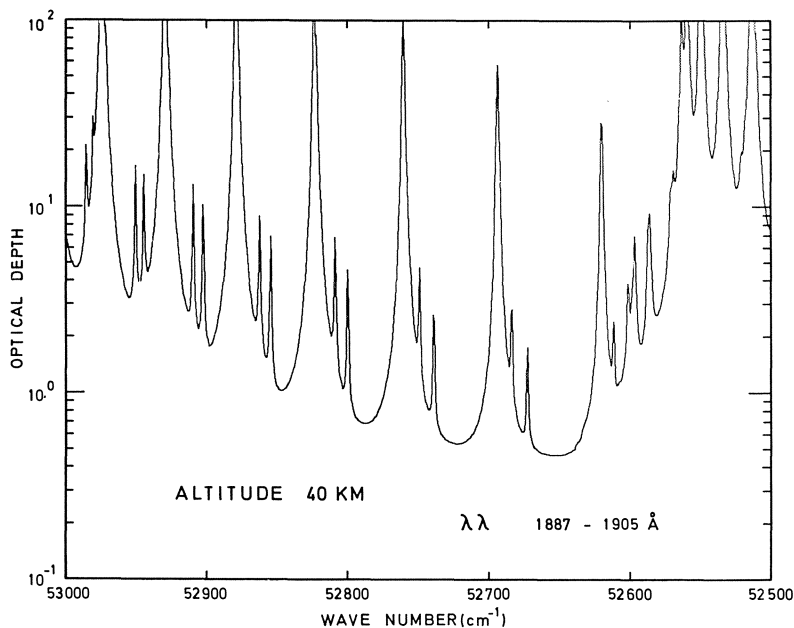


Fig. 3. Optical depth between 1887 Å and 1950 Å at 40 km. Resolution 0.5 cm^{-1} .

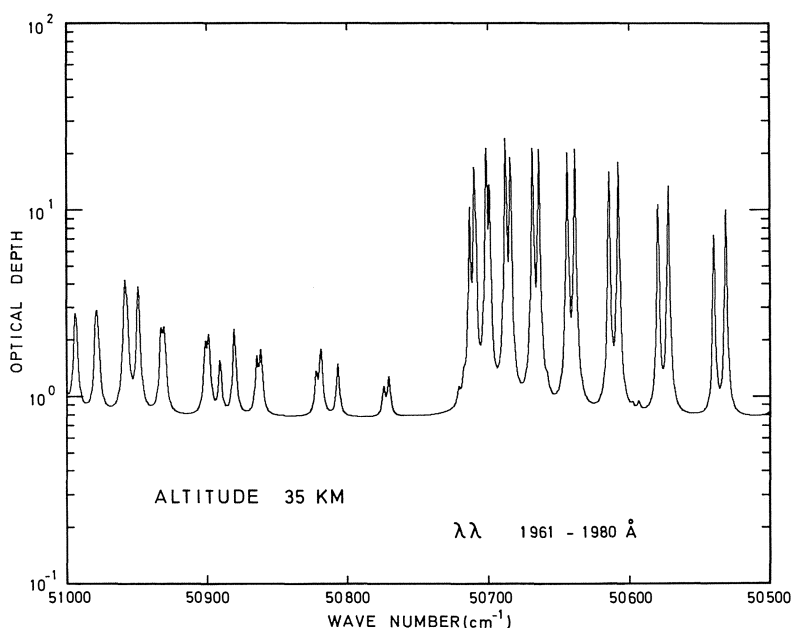


Fig. 4. Optical depth between 1961 Å and 1980 Å at 35 km. Resolution 0.5 cm^{-1} .

at 53122.79 cm^{-1} and 52561.39 cm^{-1} respectively. The smallest peaks are due to the 9-1 and 8-1 bands. At 35 km altitude, Figure 4 gives the optical depth between 1961 \AA and 1980 \AA . In this figure, the effect of the Herzberg continuum and of the ozone absorption appears clearly since there is practically a constant optical depth background of 0.8 which results from $\tau(\text{Herzberg})=0.33$ and from $\tau(\text{O}_3)=0.44$. The peaks above 50750 cm^{-1} are due to the 5-1 band and the larger peaks below 50750 cm^{-1} arise from the 2-0 band which has its band origin at 50710.83 cm^{-1} . Within a few cm^{-1} the optical depth increases from 1 to 10 and such a feature should be detectable by balloon-borne instruments with high resolution.

It is clear from Figures 2, 3 and 4 that any high resolution absorption or fluorescence experiment should take into account the fine structure of the absorption in the Schumann-Runge bands. In particular, a high resolution investigation of the absorption or emission of a minor constituent can only be performed at wavelengths where the O_2 absorption is not too high. Such a situation has been described by Jursa *et al.* (1959) in their measurements of the $\delta(0, 0)$ band of nitric oxide.

If the solar flux at the top of the atmosphere is $\Phi_i(\infty)$ in a 0.5 cm^{-1} wave number interval, the flux $\Phi_i(z)$ at altitude z is given by

$$\Phi_i(z) = \Phi_i(\infty) \exp(-\tau_i) \quad (2)$$

where τ_i is obtained by expression (1). At the present time, however, the solar flux is not known with a wave number resolution of 0.5 cm^{-1} but the reduction factor $R_i(z)$ can be defined by

$$R_i(z) = \Phi_i(z)/\Phi_i(\infty). \quad (3)$$

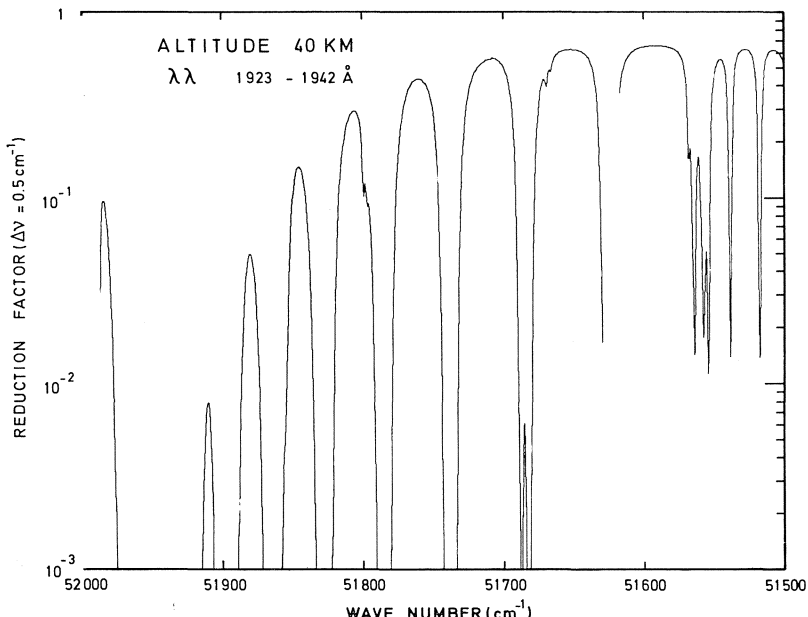


Fig. 5. Reduction factor of the solar flux between 1923 \AA and 1942 \AA at 40 km.

Figure 5 shows, as an example, the reduction factor at 40 km altitude in the wave number interval $52000\text{--}51500\text{ cm}^{-1}$. The solar flux distribution in that interval is actually modulated by the curve given in Figure 5. As a consequence of the band structure, the reduction factor $R_i(z)$ can change by more than a factor 1000 over a few cm^{-1} wave number interval.

A total reduction factor R is defined for every 500 cm^{-1} interval of Table I by the relation

$$R = \sum_{i=1}^{1000} R_i. \quad (4)$$

This reduction factor for an overhead sun is shown in Figure 6 for altitudes corresponding to the mesopause and stratopause, and down to a level of 30 km which can easily be reached by balloon-borne experiments. Although R and R_i are independent of the solar flux, the values presented in Figure 6 can however be used only when average solar fluxes are adopted over every 500 cm^{-1} wave number interval. For the 85 km values, there is a slight decrease of R between 55500 cm^{-1} and 55000 cm^{-1} ; this effect is explained by the adopted line width of 1.7 cm^{-1} (Ackerman *et al.*, 1970)

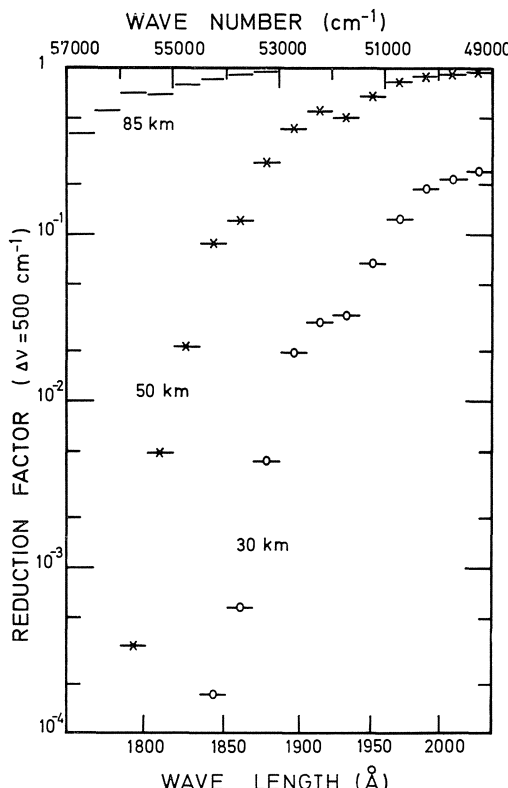


Fig. 6. Reduction factor for 500 cm^{-1} intervals at the mesopause (85 km), at the stratopause (50 km) and at 30 km.

in the 11-0 band where there is a secondary maximum of predissociation. The effect is even more pronounced at 50 km between 52000 cm^{-1} and 51500 cm^{-1} , i.e. in the 4-0 band where the maximum of predissociation corresponds to a line width of 3.7 cm^{-1} . Any increase of the line width leads, in fact, to an increase of the mean absorption in the considered band. Predissociation implies therefore an increase of the total solar flux absorption.

The solar penetration in the chemosphere depends of course on the solar flux available at the top of the atmosphere. There is at the present time some discrepancy between measured fluxes in the Schumann-Runge wavelength region. This problem has been discussed by Ackerman (1971) and his suggested values will be adopted in the present computation. Figure 7 gives the solar flux at intervals of 500 cm^{-1} for several altitudes. The solar flux $\Phi(z)$ at height z for $\Delta\nu=500\text{ cm}^{-1}$ is given by

$$\Phi(z) = \sum_{i=1}^{1000} \Phi_i(\infty) \exp(-\tau_i) \quad (5)$$

where the optical depth τ_i is computed at intervals of 0.5 cm^{-1} according to expression (1). The fluxes $\Phi_i(\infty)$ at the top of the atmosphere have been obtained by dividing Ackerman's values by 1000 in order to get fluxes in photons $\text{cm}^{-2}\text{ s}^{-1}$ for $\Delta\nu=0.5\text{ cm}^{-1}$. This procedure implies that the solar flux is constant over the 500 cm^{-1}

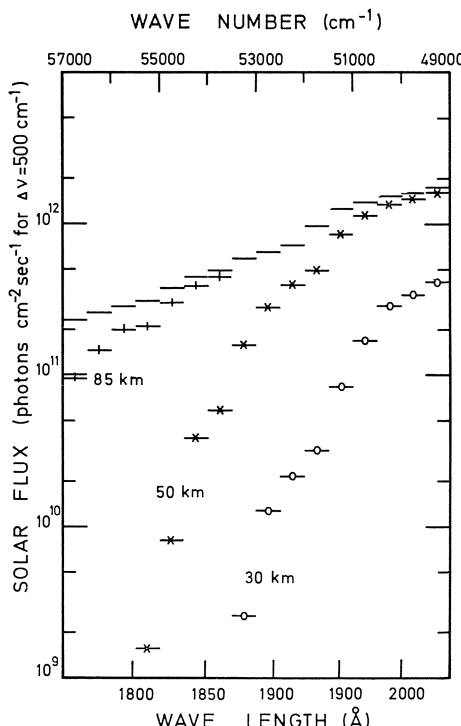


Fig. 7. Solar flux available at 85 km, 50 km and 30 km altitude.

intervals. It is, however, known that a structure exists over every 500 cm^{-1} interval, and a detailed representation of the depth of solar penetration will only be possible when the solar fluxes are available with 0.5 cm^{-1} wave number resolution. It is therefore necessary to have a digitalized solar spectrum with good absolute values and a resolution which should preferably be higher than the spectrum discussed by Brinkmann *et al.* (1966). This spectrum has not been used in the present work, since the absolute values of the ultraviolet flux have to be changed (Ackerman, 1971). The results presented in Figure 7 can nevertheless be applied to an analysis of global effects which do not require high wave number resolution.

The absorption in the Schumann-Runge bands is not only important for the atomic oxygen production rate in the chemosphere but also for the photodissociation of minor constituents such as O_3 , H_2O , CO_2 and N_2O . The photodissociation coefficient $J_i(z, X)$ in a 0.5 cm^{-1} wave number interval is given for a constituent X by

$$J_i(z, X) = K_i \Phi_i(z) \quad (6)$$

where $\Phi_i(z)$ is given by (2) and K_i is the photodissociation cross section for the constituent X . For every 500 cm^{-1} interval of Table I, the photodissociation coefficient is simply

$$J(z, X) = \sum_{i=1}^{1000} J_i(z, X). \quad (7)$$

The total photodissociation coefficient over the Schumann-Runge bands is then obtained by summing the $J(z, X)$ values given by (7).

The molecular photodissociation coefficient in the Schumann-Runge system depends of course on the existence of predissociation. According to Flory (1936) and to Hudson and Carter (1969), the upper vibrational levels with $v' > 2$ of the excited $B^3\Sigma_u^-$ electronic state are subject to predissociation. The measurements by Feast (1949) indicate no predissociation for the bands with $v' = 3$. Ackerman and Biaumé (1970) have, however, determined a total rotational line width of the order of 1 cm^{-1} in the $v' = 0, 1$ and 2 bands. Considering that the total Doppler broadening at 2000 \AA is of the order of 0.1 cm^{-1} for a temperature of 300 K , it can be suggested from the measurements of Ackerman and Biaumé (1970) that predissociation occurs even for $v' \geq 0$. Therefore, in the wavelength region where predissociation is taken into account, the photodissociation cross section K_i is composed of two terms: a contribution from the Schumann-Runge bands, and one from the Herzberg continuum which also leads to the production of $\text{O}({}^3P)$ atoms. In order to show the effect of predissociation starting at $v' = 0$ or at $v' > 3$, Table III gives the O_2 photodissociation coefficients in the Schumann-Runge bands computed for the two cases. The last column is the total photodissociation coefficient due to Lyman α , to the Schumann-Runge continuum, to the Schumann-Runge bands and to the Herzberg continuum. The total value of $J(\text{O}_2)$ has been computed with predissociation for $v' > 3$. When complete predissociation occurs in the Schumann-Runge bands, Table III shows that $J(\text{O}_2)$, given in the last column, has to be multiplied by a factor 1.08 at 60 km . Above and below this altitude the difference between the values of $J(\text{O}_2)$ for total predissociation and for

TABLE III
Photodissociation coefficient (s^{-1}) for O_2

$z(\text{km})$	$J(\text{S-R})$ Predissociation $v' \geq 0$	$J(\text{S-R})$ Predissociation $v' > 3$	$J(O_2)$
100	9.14×10^{-8}	9.14×10^{-8}	3.77×10^{-7}
95	6.35	6.32	1.56
90	3.65	3.62	5.45
85	1.76	1.73	2.14
80	9.07×10^{-9}	8.80×10^{-9}	1.18
75	4.66	4.40	6.50×10^{-9}
70	2.59	2.35	3.72
65	1.47	1.29	2.46
60	8.99×10^{-10}	7.47×10^{-10}	1.90
55	5.73	4.52	1.57
50	3.38	2.53	1.27
45	2.06	1.51	9.41×10^{-10}
40	1.19	8.88×10^{-11}	5.25
35	5.47×10^{-11}	4.45	2.14
30	2.05	1.79	7.24×10^{-11}

predissociation for $v' > 3$ decreases and becomes of the order of 1% at the mesopause. Despite the fact that there is some evidence for total predissociation, the slightly lower values $J(O_2)$ are adopted, since the absolute values of the solar flux are not known with sufficient accuracy and also since the difference between the two possibilities does not lead to very important changes in the total photodissociation coefficient.

As an example, Figure 8 gives the fine structure of the photodissociation coefficient of O_2 between 1905 Å and 1923 Å. This wavelength interval has been chosen since there is no great variation in the structure of the solar radiation according to Brinkmann *et al.* (1966). The dashed line in Figure 8 gives the mean value for $J(O_2)$ over the considered 500 cm^{-1} interval. Some smooth minima appear in Figure 8, particularly below $52\,300 \text{ cm}^{-1}$. These features are due to the combined effect of the reduction factors R_i and the photodissociation cross sections K_i which are multiplied by each other in the photodissociation coefficients. At certain wavelengths, the decrease of the reduction factor R_i is compensated by the cross section K_i appearing in front of the exponential term. It will not be possible to present physically significant curves like that of Figure 8 until the solar spectrum is known with greater resolution than at present.

It is interesting to compare the present photodissociation coefficient of O_2 in the Schumann-Runge bands with the values deduced by Hudson *et al.* (1969) from their laboratory absorption measurements. It can be seen in Figure 9 that the agreement is quite satisfactory when the molecular oxygen total content varies between 10^{17} cm^{-2} and 10^{21} cm^{-2} . These values correspond roughly to the height region between 100 km and 60 km. In order to obtain a significant comparison, the computation presented in Figure 9 has been made using the solar fluxes of Brinkmann *et al.* (1966) averaged over the 500 cm^{-1} wave number intervals of Table I.

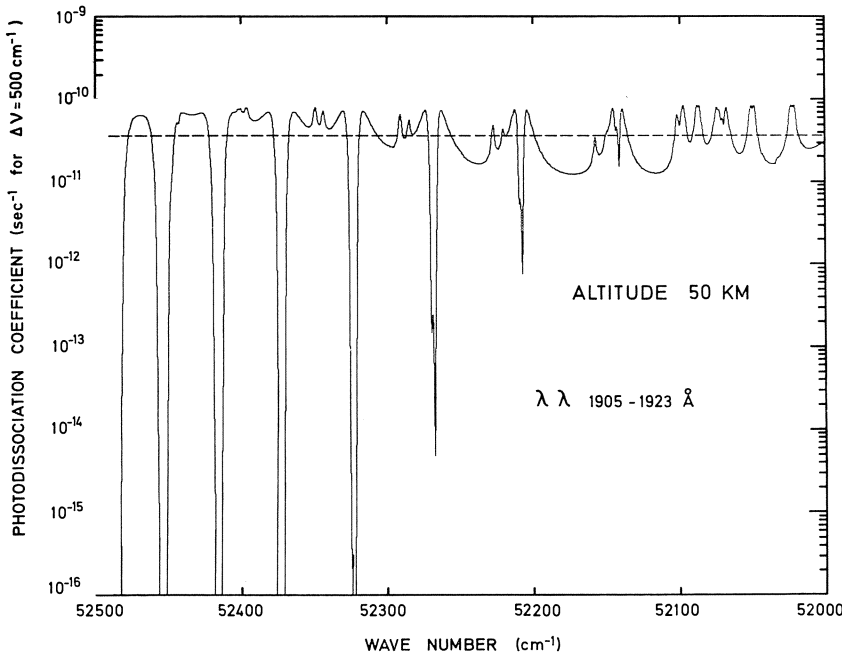


Fig. 8. Example of the structure of the molecular oxygen photodissociation coefficient at 50 km altitude between 1905 Å and 1923 Å.

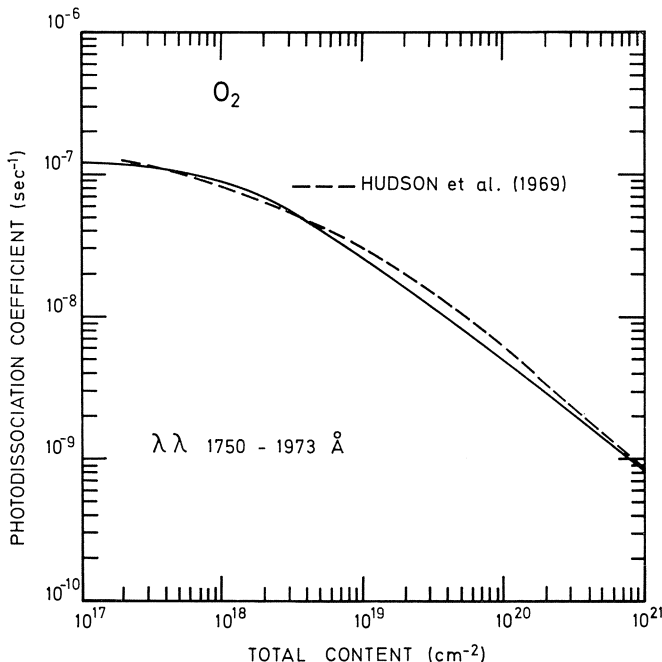


Fig. 9. Comparison between the calculated photodissociation coefficient of molecular oxygen for the spectral range 1750 Å-1973 Å and the values given by Hudson *et al.* (1969) between 2×10^{17} and 10^{21} molecules cm^{-2} .

The photodissociation rate of molecular oxygen depends on the whole solar spectrum of $\lambda < 2424 \text{ \AA}$. The importance of the Schumann-Runge bands is shown in Figure 10 where the total photodissociation rate is represented as well as the contribution due to the wavelength region between 1754 \AA and 2020 \AA . Between approximately 60 km and 90 km altitude, the predissociation in the Schumann-Runge bands is the major process responsible for O_2 dissociation for overhead sun conditions.

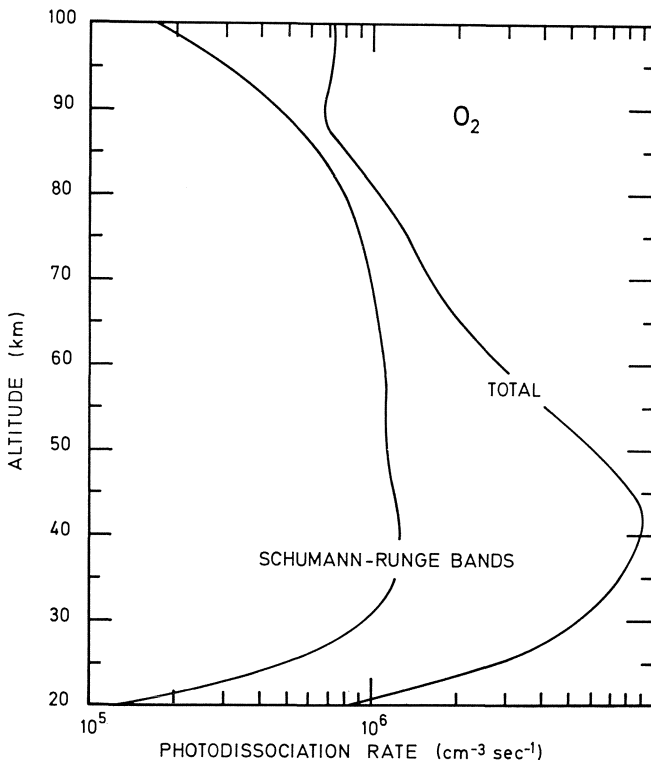


Fig. 10. O_2 photodissociation rate. Contribution of the Schumann-Runge bands region is important between 90 km and 60 km.

For practical calculations, it would be useful to have a set of mean absorption cross sections which could give results similar to the detailed computation described previously. In every 500 cm^{-1} wave number interval of Table I, it is possible to define a mean absorption cross section σ_m by the relation

$$\sigma_m = \frac{\sum \sigma_i \exp(-\tau_i)}{\sum \exp(-\tau_i)} \quad (7)$$

where the sums extend over the 1000 values included in the interval considered. The mean absorption cross sections obtained in this way are altitude dependent. Figure 11 shows σ_m versus wave number for different values of the total optical depth and it is

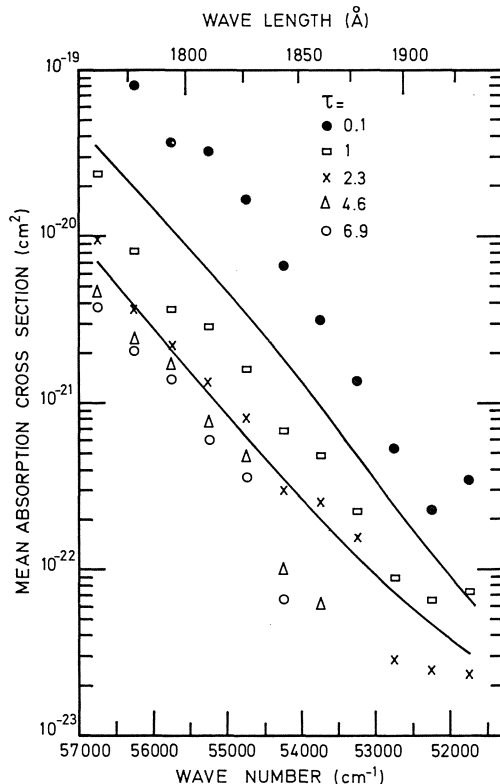


Fig. 11. Mean absorption cross sections for $\Delta\nu = 500 \text{ cm}^{-1}$ and for different values of the optical depth τ .

seen that σ_m decreases with increasing optical depth. The squares in Figure 11, corresponding to unit optical depth, clearly show three plateaux which are located in the bands where a maximum of predissociation occurs, i.e. at $v' = 4, 7$ and 11 . This feature is also visible in Figure 6 showing the reduction factor.

From Figure 11 it is not possible to deduce a general law which is sufficiently precise for the exact representation of the variation of σ_m with wave number and with height. However, the two solid curves H and L of Figure 11 are an attempt to represent the mean absorption cross section for optical depths between 0 and 1 and for greater values of τ . In order to discuss the validity of this choice, Figure 12 gives the molecular oxygen photodissociation coefficient in the Schumann-Runge bands computed using the two sets of values. Curve H corresponds to the high values of Figure 11 and curve L corresponds to the low values. An analysis of Figure 12 indicates that the high values used by Nicolet (1970) give the best agreement with the exact computation represented by the full line. There is, however, a slight underestimation of the total photodissociation coefficient near 90 km when curve H is adopted. But the low values L cannot be used above 70 km for computing $J(\text{O}_2)$.

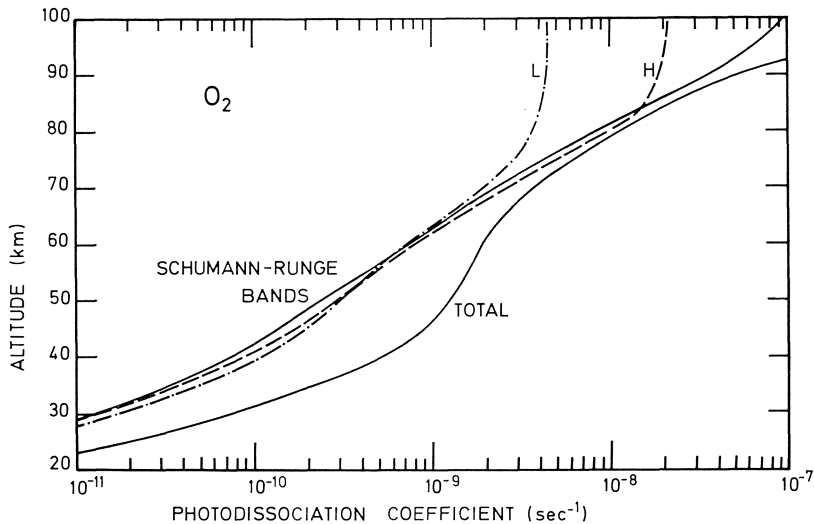


Fig. 12. Molecular oxygen photodissociation coefficient computed for low (L) and high (H) values of the mean absorption cross sections. The total $J(O_2)$ corresponds to the detailed computation (solid line) in the Schumann-Runge bands.

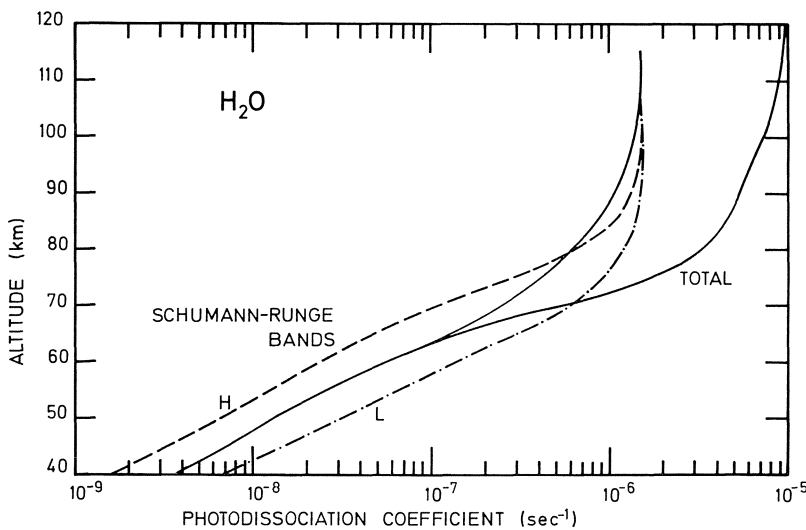


Fig. 13. Water vapour photodissociation coefficient computed for low (L) and high (H) values of the mean absorption cross sections. The total value corresponds to the detailed computation in the Schumann-Runge bands which give the major contribution below 70 km altitude.

It is now necessary to investigate the effect of the high and low values of σ_m on the photodissociation coefficients of minor constituents such as H_2O , CO_2 , O_3 and N_2O , since the mean absorption cross section is not identical with the photodissociation cross sections K_i of Equation (5). Figure 13 shows the photodissociation coefficient for water vapour. Down to the lower mesosphere, Lyman α makes an important contribu-

tion to $J(\text{H}_2\text{O})$ (Nicolet, 1970, 1971); the total $J(\text{H}_2\text{O})$ is also shown in Figure 13 in order to indicate where the Schumann-Runge bands become the major component. The curve L and H correspond to the mean cross sections L and H of Figure 11. It is clear that neither the low values nor the high values can fit the detailed computation indicated by the solid curve. The low values (curve L) overestimate $J(\text{H}_2\text{O})$ by a factor of 2 and the high values (curve H) underestimate $J(\text{H}_2\text{O})$ by a factor of 2 below 70 km where the Schumann-Runge bands produce the major contribution to the total photodissociation coefficient. The comparison between Figures 12 and 13 indicates that it is not possible to adopt a unique set of mean absorption cross sections which simultaneously fit the effective dissociation coefficients of O_2 and of the minor constituents. It is therefore more suitable to use the reduction factors R described earlier for a computation of the different photodissociation coefficients for minor constituents. Moreover, the reduction factors can be adapted to any degree of resolution of the solar spectrum. It should however be pointed out that in the present work all the computations are made for an overhead sun and the reduction factors of Figure 6 cannot be applied to other zenith angles without recomputing all the fine structure reduction factors R_i .

High resolution absorption cross sections are now available for molecular oxygen in the Schumann-Runge band system. Since the cross sections are temperature dependent, the absorption of solar radiation is a function not only of the total content of the absorbing species but also of the atmospheric temperature.

The great variability of the optical thickness as a function of wavelength implies that any high resolution experiment designed should take into account the possibility of changes by a factor 100 in the optical depth over a very small wave number interval. A detailed study of the solar radiation absorption will be possible only when the solar spectrum is known with a better resolution. However it is possible at present to investigate the average solar penetration by means of the reduction factors which are independent of both the absolute value and the fine structure of the solar flux. The reduction factors show the line broadening effect related to the predissociation in the Schumann-Runge bands.

The comparison between the values of the exact photodissociation coefficients and those obtained with different mean cross sections shows that it is not possible to reconcile these values with a unique set of mean cross sections. This is due to the fact that the mean absorption cross section depends on the optical depth, i.e. on the altitude. A calibration must be made in each case in order to determine, in the spectral region of the Schumann-Runge bands, the mean absorption cross section which must be adopted. Finally, another investigation will be necessary in order to study the effect of various solar zenith angles.

Acknowledgement

I would like to express my gratitude to Prof. M. Nicolet for his valuable advice during the preparation of this work.

References

- Ackerman, M.: 1971, this volume, pp. 149–59.
- Ackerman, M. and Biaume, F.: 1970, *J. Mol. Spectr.* **35**, 73–82.
- Ackerman, M., Biaume, F., and Nicolet, M.: 1969, *Can. J. Chem.* **47**, 1834–40.
- Ackerman, M., Biaume, F., and Kockarts, G.: 1970, *Planetary Space Sci.* **18**, 1639–51.
- Brinkmann, R. T.: 1969, *J. Geophys. Res.* **74**, 5355–68.
- Brinkmann, R. T., Green, A. S., and Barth, C. A.: 1966, 'A Digitalized Solar Ultraviolet Spectrum', Technical Report No. 32–951, Jet Propulsion Laboratory, Pasadena, California.
- Feast, M. W.: 1949, *Proc. Phys. Soc.* **A62**, 114–21.
- Flory, P. J.: 1937, *J. Chem. Phys.* **4**, 23–7.
- Hudson, R. D. and Carter, V. L.: *Can. J. Chem.* **47**, 1840–4.
- Hudson, R. D., Carter, V. L., and Breig, E. L.: 1969, *J. Geophys. Res.* **74**, 4079–86.
- Jursa, A. S., Tanaka, Y., and Le Blanc, F.: 1959, *Planetary Space Sci.* **1**, 161–72.
- Nicolet, M.: 1964, *Disc. Faraday Soc.* **37**, 7–20.
- Nicolet, M.: 1970, *Ann. Geophys.* **26**, 531–46.
- Nicolet, M.: 1971, this volume, pp. 1–51.